ARTICLE IN PRESS

Journal of Atmospheric and Solar-Terrestrial Physics xxx (xxxx) xxx–xxx

Contents lists available at ScienceDirect

Journal of Atmospheric and Solar-Terrestrial Physics

journal homepage: www.elsevier.com/locate/jastp

Reprint of A deterministic model for forecasting long-term solar activity☆

Eleni Petrakou[1]

Athens, Greece

ARTICLE INFO

Keywords:
Solar cycle
Solar flares
Forecasts

ABSTRACT

A phenomenological model is presented for the quantitative description of individual solar cycles' features, such as onset, intensity, evolution, in terms of the number of M and X-class solar flares. The main elements of the model are the relative ecliptic motion of the planets Jupiter and Saturn, and its synergy with a quasi-periodic component of solar activity. Using as input the temporal distribution of flares during cycle 21, the general evolution of cycles 22–24 is reproduced in notable agreement with the observations, including the resurgence of activity in the last months of 2017, and further predictions are provided for cycle 25. This deterministic description could contribute to elucidating the responsible physical mechanisms and forecasting space weather.

1. Introduction

Energetic solar events and the quasi-periodic variability in solar activity, known as the solar cycle, are widely attributed to the Sun's magnetic dynamo mechanism (Parker, 1955; for a recent review, Brun and Browning, 2017); however their modelling is still far from complete (e.g. Spruit, 2010; Brun and Browning, 2017) and no regulating factors have been established. Existing methods for the prediction of the timing and amplitude of solar cycles mainly depend on extrapolations from sunspot numbers or geomagnetic precursors (e.g. Hathaway et al., 1994, 1999), becoming available only very close to or after a cycle's start and often departing from the actual events (Usoskin and Mursula, 2003; Pesnell, 2008; Hathaway and Wilson, 2006; NOAA, 2009), although recently proxies like the solar background magnetic field enable new approaches (e.g. Zharkova et al., 2015). In the current article a deterministic model is presented for the quantitative description of the cycles' evolution, in terms of the number of M and X-class solar flares. Section 2 presents the used data and conventions; the derivation of the model and its results and predictions are presented in Section 3, with a brief discussion found in Section 4. A preliminary form of this work first appeared in February 2017 (Petrakou, 2017).

2. Data and conventions

The observable of choice in studies of the solar cycle has traditionally been sunspots, however the last four decades made possible the daily recordings of solar flares. While sunspots are indirect indicators of underlying dynamics, flares constitute actual physical events with definite timing and energy, as well as impact on space weather, and this study will focus on them. In the current article M-class and X-class flares (covering X-ray brightness of 10^{-5} W/m^2 and above) are used; only the counts of these flares are examined, treating them as statistical timed events, while less energetic flares which occur in large numbers almost daily are not included. However, the use of C-class flares and brightness is discussed towards the end of Section 3.

Solar flares data comprise the X-ray flux measurements of the NOAA SMS and GOES satellites and are provided by the USA National Oceanic and Atmospheric Administration (NOAA, 2017). Data on sunspots come from the archives of the Royal Observatory of Belgium (SILSO, 2017).

The presented model was developed using the data since the start of cycle 21 and up to the end of year 2016, in total 6339 and 491 M and X-class flares, with the two categories corresponding to X-ray brightness of 10^{-5}-10^{-4} W/m^2 and all higher values, respectively. A corresponding definition is used for the cycle start and end (instead of the customary sunspot cycle). The start of each cycle is defined by the date of the first M-class flare erupting from a sunspot of reversed magnetic polarity (these flares are also the first ones after the minimum in flare activity, and they come after the minimum in sunspot activity, although in two of the cases they are not the first ones after the latter). The resulting start dates for cycles 21–24 are: 1977/01/31, 1986/10/19, 1997/04/01, 2010/01/19. The end of each cycle is defined by the start of the next one.

DOI of original article: https://doi.org/10.1016/j.jastp.2018.04.009

☆ The is a re-publication of "A deterministic model for forecasting long-term solar activity" published in volume 175, pages 18-23. This paper is part of the present special issue Future Solar Activity. The publisher apologizes for the error. http://dx.doi.org/10.1016/j.jastp.2018.06.010.

E-mail address: eleni@petrakou.net.

[1] On leave from the Center for Axion and Precision Physics Research, Institute for Basic Science, Republic of Korea.

https://doi.org/10.1016/j.jastp.2018.06.010
Received 2 January 2018; Received in revised form 4 April 2018; Accepted 19 April 2018

Please cite this article as: Petrakou, E., Journal of Atmospheric and Solar-Terrestrial Physics (2018), https://doi.org/10.1016/j.jastp.2018.06.010

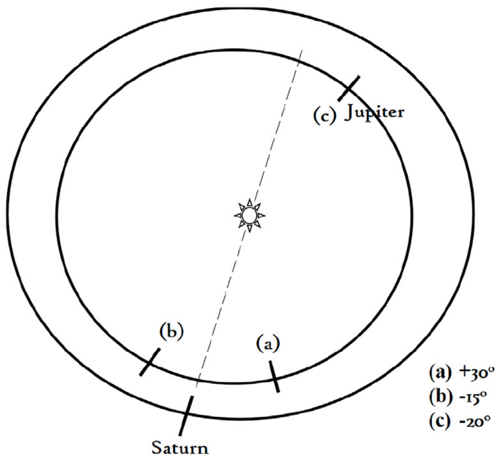

Fig. 1. Examples of the planetary relative angle convention.

All quoted angles will refer to the relative heliocentric ecliptic longitude between Jupiter and Saturn (HelioWeb, 2017). With the exception of Fig. 2, both conjunction and opposition are set equal to zero degrees, thus the range of values is [-90°, 90°]. Fig. 1 illustrates three examples of the relative angle. In this convention, "91°" is actually −89°, since the closest alignment is the next opposition.

3. Observations and calculation

The model is initiated by the empirical observation that solar activity in terms of energetic flares tends to peak around the dates of alignment of Jupiter and Saturn, and be bound within the surrounding range roughly defined by the dates of their quadrature (Fig. 2a). However, as we progress from cycles 21 to 24 the activity is "dragged" further away from the alignment towards later dates (Fig. 2b). As this lagging is compatible with the staggering between the two planets' synodic period and the observed solar cycles duration of ~11 years, it can be asked whether the evolution of solar activity is the coupled effect of two contributions: an internal mechanism generating the 11-year cycle, presumably of magnetic origin, and a triggering associated with the approach and retreat of Jupiter and Saturn.

This proposition can be quantified by assuming that the effects of each contribution can be expressed by a Gaussian distribution with known mean and roughly known standard deviation: the distribution corresponding to the internal component would be centered on the temporal middles of cycles and span somewhat less than 11 years; and the distribution corresponding to the "Jupiter-Saturn component" would be centered on the dates of their alignments and lie mostly between −45° and +45° with respect to the alignments (the last requirement stemming empirically, Fig. 2). Noting that in cycle 21 the dates of the temporal middle and of the alignment happened to lie close (237 days away), it will be assumed that during that cycle the full deployment of the two effects can be observed. This enables the extraction of the two distributions from the data of cycle 21, by finding two Gaussian functions which satisfy the described bounds for the mean and the standard deviation, and follow the envelope of the recorded activity within each component's respective time span (Fig. 3). The two resulting functions' constants are close and they were refitted with equal values (fits performed with the ROOT package, Brun and Rademakers, 1997). The parameters of the two distributions are $\{\mu, \sigma, c\} = \{0{,}670{,}190\}, \{-237{,}510{,}190\}$.

By expanding over the time range of the latest four cycles and repeatedly placing the two distributions at the relevant dates, i.e. centering the Jupiter-Saturn distribution on the dates of alignments and the internal distribution on the temporal middles of cycles, Fig. 4 a is obtained. On average, the distance between these two dates increases by 396 days between consecutive cycles (given the synodic half-period average of 3634 and the sunspot cycle average of 4030 days); this number was used for estimating the temporal middle for the ongoing cycle 24, with respect to 23. The model is completed by the assumption that the coupling of the two components is expressed by their common area, shown as a binned histogram in Fig. 4 a. The assumptions used in this construction (the use of M and X-class flares, relevant cycle timing, the presence of two components, the modeling by Gaussian functions with the assumed span and timing, their extraction from cycle 21, their coupling) form the set of hypotheses to be tested against the data.

The last distribution is proposed to describe the long-term solar activity in terms of energetic flares; in Fig. 4 b it is overlayed with the observations up to the end of year 2016, including systematic uncertainties from the binning choices and from the timing of cycle 24 (Appendix A). Notable agreement can be seen in general features such as start and time span of activity, intensity, and evolution of each cycle. Short-term departures need to be understood in more depth, more prominent ones being the excess in the descending phase of the two latest cycles. However, certain short-term features which are generally considered puzzling (e.g. Hathaway, 2015) are present in the model, such as the deep minimum and late onset of cycle 24, and the abrupt decrease in activity after the year 2015 (with the two planets retreating further than +90° in December 2015, marking the pause of activity before a new build-up begins with their approach).

For clarity, it can be pointed out that the width of the internal distribution is not meant to correspond to the duration of the sunspot cycle, or any other solar activity cycle, but is a measure of the span of the internal component's influence. Although the main coverage of these distributions is taken as fixed, their central dates vary to follow

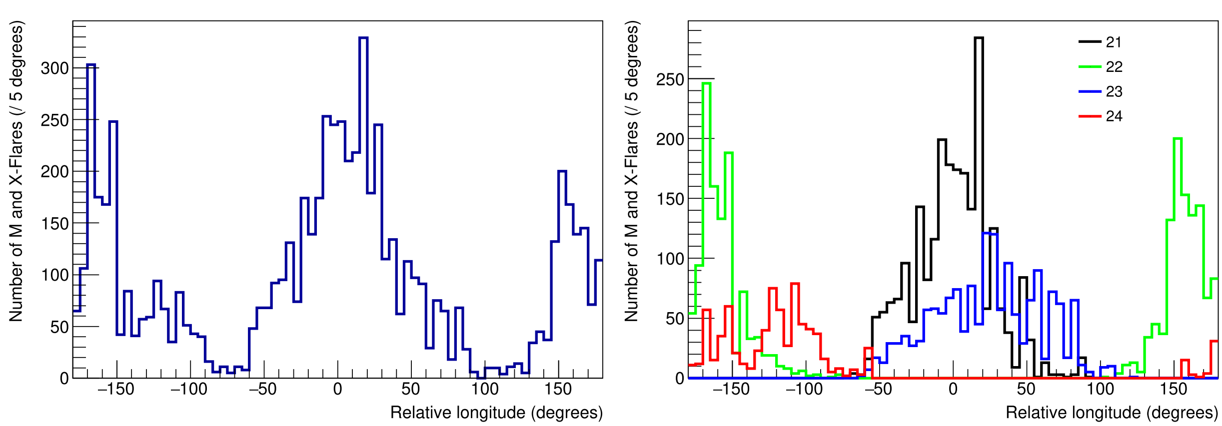

Fig. 2. Solar flares – planetary angular relation. Number of M and X-class flares of cycles 21–24 up to the end of year 2017, as a function of the relative ecliptic longitude between Jupiter and Saturn, (a) collectively and (b) individually for each cycle (see text for definition of cycle start and end).